Food Chemistry: X 22 (2024) 101288

Contents lists available at ScienceDirect

Food Chemistry: X

journal homepage: www.sciencedirect.com/journal/food-chemistry-x

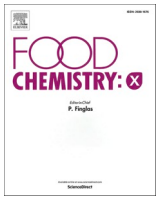

Formation of special odors driven by volatile compounds during the growth and maturation in edible fungi (*Phallus impudicus*)

Huijuan Liu [a], Zhifei Cheng [b], Jiao Xie [a,*]

[a] *The Key Laboratory of Environmental Pollution Monitoring and Disease Control, Ministry of Education, School of Public Health, Guizhou Medical University, Guizhou 561113, PR China*

[b] *Basic Teaching Department, Guizhou Vocational College of Agriculture, Guizhou 551499, PR China*

ARTICLE INFO

Keywords:
Edible fungi of *Phallus impudicus*
Volatile compounds
Growth stages
HS-SPME-GC–MS

ABSTRACT

Composition and content of volatiles, the important factors in flavor formation of edible fungi, are affected by growth process. GC–MS was performed and a total of 102 volatiles were identified in *Phallus impudicus*. Almost all identified volatile compounds showed an obvious upward trend at four growth period, and reached the maximum at fourth stage (PIII), of which the transition from first stage (ZP) to second stage (PI) achieved a breakthrough for 88 volatile compounds from scratch. The PCA and HCA results showed that the four stages were completely separated and appeared different, among which third stage (PII) and PIII might be the two dramatic change nodes in aroma quality. In addition, the top 50 differential metabolites were screened by OPLS-DA and PLS-DA, and correlation analysis showed that 6-undecyl alcohol, α-terpine-7-al, 2, 4-decenol, and 2-cyano-2-ethyl-butanamide, might co-regulate the flavor formation of *Phallus impudicus* through synergistic action of other chemical components.

Introduction

Phallus impudicus (*Phallus impudicus* L. ex. Pers.), known as "Wuqunsun" in China, is a genus of edible fungus homologous to medicine that belongs to the family of *Phallus*, class of Phallaceae and oder of Phallales (Hosaka et al., 2006; Khan et al., 2020; Pudil, Uvira & Janda, 2014; Shou, 2020). The mature fruiting body of *Phallus impudicus* consists mainly of three parts, namely pileus (covered with spores), volva and stipe (Pudil, Uvira & Janda, 2014). Of them, the commercially available product generally takes the stipe as edible part. Previous studies have shown that *Phallus impudicus* is rich in polysaccharides, polyphenols, flavonoids, and other bioactive substances, which have significant effects on immune regulation, anti-oxidation, lowering blood lipid and inhibiting tumor. (Gupta, Jayaprakash & Shinde, 2016; Khan et al., 2020; Kuznecova, Jegina, Kuznecovs & Kuznecovs, 2007; Shou, 2020; Vyacheslav et al., 2019; Zhang, 2015). Thus, *Phallus impudicus* has good commercial value and social value.

At present, the *Phallus impudicus* was well known not only the high nutritional value but also its unique flavor (Gupta et al., 2016; Shou, 2020). Of them, flavors was strictly affected by the composition and abundance of volatile compounds (Gupta et al., 2016; Pudil, Uvira & Janda, 2014). Currently, the most studies on volatile compounds have mainly focused on widely cultivated and consumed fungi such as *Agaricus bisporus* and *Shiitake Mushrooms* in the market (Cho, Seo & Kim, 2003; Feng et al., 2021; Li et al., 2022; Yao et al., 2023). For example, existing studies have pointed out that both eight carbon compounds (1-octanol, 3-octanol, 3-octanone, etc.) and some non-eight carbon compounds (*N*-nonanal, etc.) were important volatile components in these edible fungi (Feng et al., 2021). However, there are few studies on the changes of volatile components in *Phallus impudicus*. As a crucial factor for consumer preferences, the special flavor of edible fungi was also mainly affected by growth process (Aisala, Sola, Hopia, Linderborg & Sandell, 2019; Cao et al., 2023; Grosshauser & Schieberle, 2013; Tietel & Masaphy, 2018; Yao et al., 2023). In addition, the unique volatile compounds in each type of edible fungi contributed to the unique aroma and participated in the regulation of edible fungi growth (Aisala, Sola, Hopia, Linderborg & Sandell, 2019; Cao et al., 2023; Dickschat, Celik & Brock, 2018; Yao et al., 2023). Therefore, the factor of maturity can significantly affect the composition and abundance of volatile compounds (Cho, Seo & Kim, 2003; Feng et al., 2021; Hou, Liang & Wang, 2020; Pudil, Uvira & Janda, 2014; Xie, Cao, Wang, Zhang & Deng, 2023). All in all, the changes of volatile compounds during the

* Corresponding author at: the key Laboratory of Environmental Pollution Monitoring and Disease Control, Ministry of Education, Guizhou Medical University, GuiZhou 550025, PR China.
E-mail address: lxj4516@126.com (J. Xie).

https://doi.org/10.1016/j.fochx.2024.101288
Received 20 November 2023; Received in revised form 1 March 2024; Accepted 11 March 2024
Available online 15 March 2024

development and maturation reflect the variations in flavor of edible fungi during this period, and these characteristic changes can be used as important indicators of maturity and optimal harvest time of edible fungi.

At present, previous studies have revealed that the flavor formation of edible fungi was affected by the development stage (Aisala, Sola, Hopia, Linderborg & Sandell, 2019; Cao et al., 2023; Dickschat et al., 2018; Grosshauser & Schieberle, 2013; Tietel & Masaphy, 2018; Yao et al., 2023). However, little is known about the effects of different developmental stages on volatile constituents related to flavor formation in the rare edible fungi, *Phallus impudicus*.. In this study, the samples of *Phallus impudicus* at four different developmental stages were collected, headspace solid-phase microextraction-gas chromatography-mass spectrometry (HS-SPME-GC–MS) was performed to analyze the stage-dependent changes of volatile constituents, and the key volatile compounds in the stipes of four growth stages were screened by combining

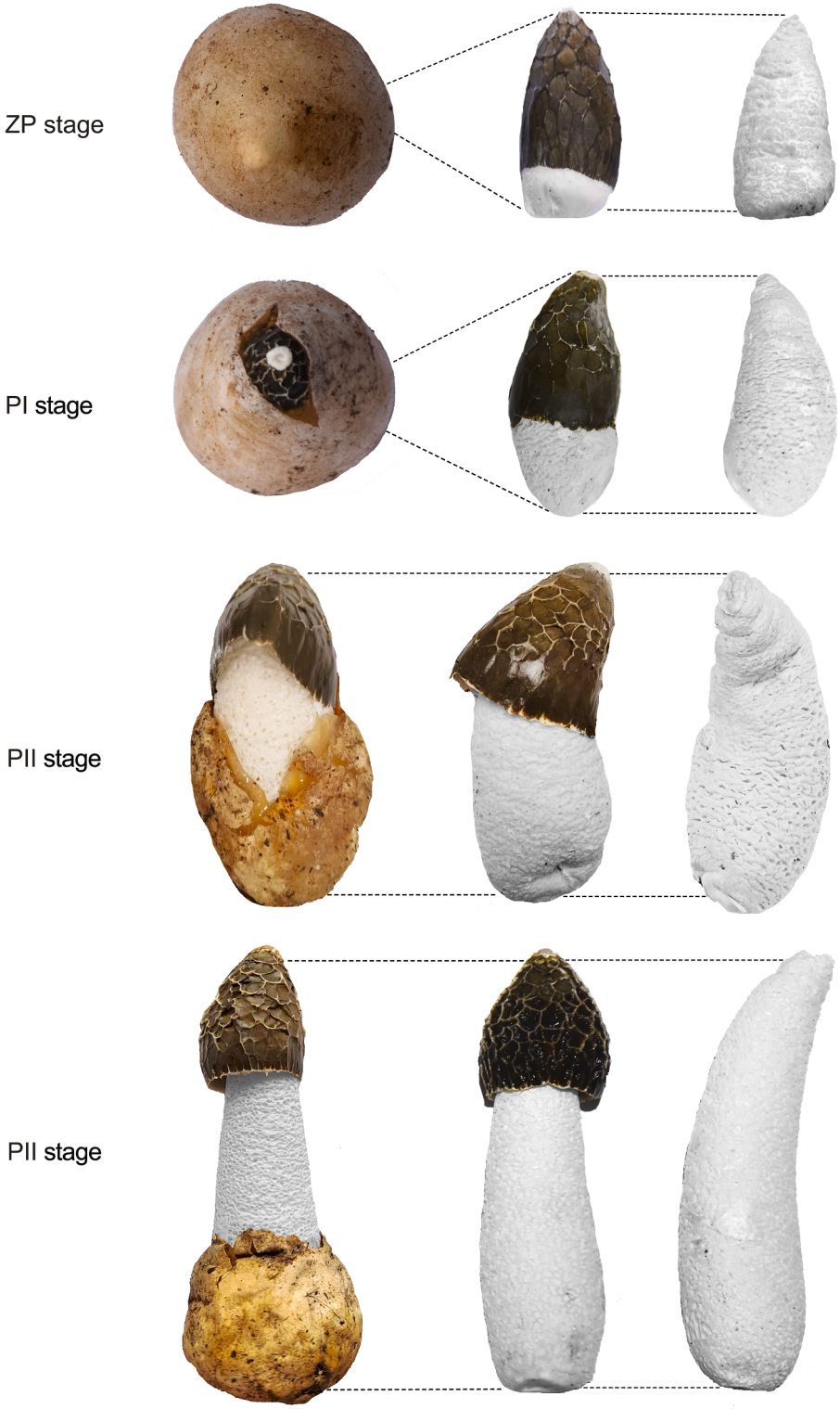

Fig. 1. Schematic diagram of *Phallus impudicus* at different developmental stages (ZP, PI, PII and PIII stage).

orthogonal partial least squares-discriminant analysis (OPLS-DA) and partial least squares-discriminant analysis (PLS-DA). Through the in-depth study of the characteristic volatile constituents of *Phallus impudicus*, the theoretical basis for the chemical features behind the formation of the special flavor and the best harvest time of *Phallus impudicus* was provided.

Materials and methods

Plant materials

Phallus impudicus samples used in the present study originated from a under-forest planting field in Baiyun District, Guiyang City, Guizhou Province, China. The development period in this study was divided into four stages (Immature egg form for ZP, Shell breaking stage for PI, Rapid growth stage for PII and Mature stage for PIII) showed in Fig. 1. Five strains of *Phallus impudicus* were selected for each developmental stage, and fifteen stipes were collected. A total of three biological replicates were performed in this study. The samples used were the same size and appearance at the same developmental stage with free from pests or diseases as well as mechanical damage. After the sample collection, the volva, stipe and pileus were separated immediately to prevent the cross-contamination between different parts or the fuzzy stage division caused by the failure to terminate the growth in time. Of them, the stipes were immediately placed in liquid nitrogen, and then stored at −80 °C until extraction.

Chemicals and reagents

Sodium chloride was of analytical grade and was supplied by Sinopharm Chemical Reagent Co., Ltd (Shanghai, China). Chromatographic grade *n*-hexane was acquired from Merck Co (Darmstadt, Germany). The internal standard of [3,4,5,6-2H4]-Methyl 2-hydroxybenzoate and standards of 102 compounds listed in Table 1were all chromatographic grade, and part of them were purchased from BioBioPha/WAKO/Sigma-Aldrich (St Louis, MO, USA).

Extraction of volatile components

The extraction method was referred to the study of Hou, Liang and Wang (2020) on volatile compounds of navel orange and modified. The stipe samples of the four developmental stages taken out from the refrigerator at −80 °C was immediately placed in liquid nitrogen and ground into powder. Approximately 500 mg of powder sample was extracted by 2 mL of saturated sodium chloride solution with 10 μL of [3,4,5,6-2H4]-Methyl 2-hydroxybenzoate (50 μg/mL) as internal standard were added. Subsequently, the volatile compounds from the stipe of *Phallus impudicus* were extracted using the Headspace-Solid Phase Microextraction (HS-SPME), i.e., the HS vial with mixed liquor was shaken at 60 °C for 5 min, then extraction was conducted using a 120 μm

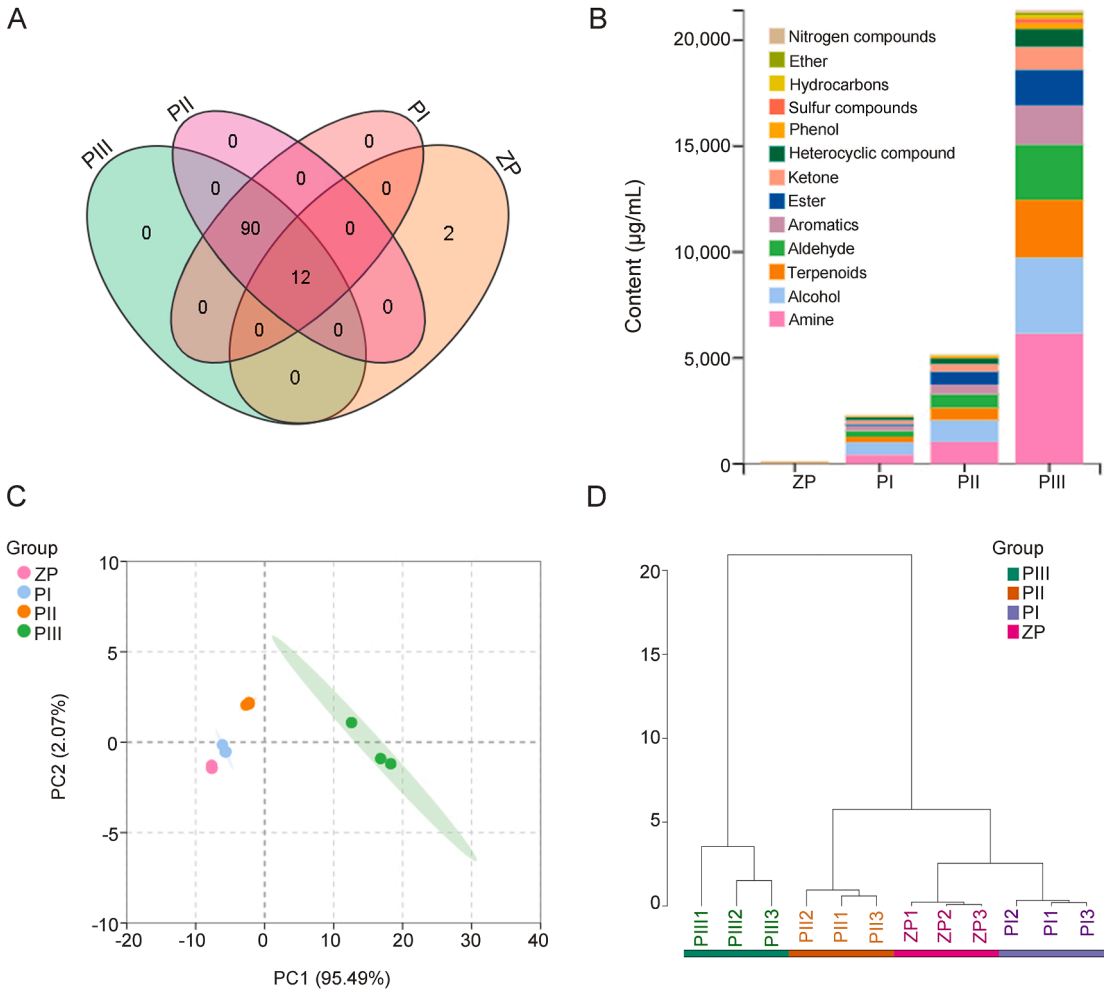

Fig. 2. Types and multivariate statistical analysis of volatile compounds in *Phallus impudicus* at different development stage (ZP, PI, PII and PIII stage). (A) indicated Venn diagram; (B) exhibited the classification and relative content of volatile compounds; (C) meant the principal component analysis (PCA). (D) indicated the hierarchical cluster analysis (HCA).

Table 1
Volatile compounds of *Phallus impudicus* with various developmental stages.

NO.	Compounds	Identification of the volatile components							Relative contents (μg/mL)			
		RRI	RI	CAS	Q1	Q2	M (Da)	IB	ZP	PI	PII	PIII
1	iminodiacetonitrile	–	1108	628–87-5	94	68	95.05	MS	0.00 ± 0.00^{a}	3.11 ± 0.28^{a}	7.54 ± 1.49^{a}	58.31 ± 10.72^{c}
2	geranylacetone	1449	1453	3796–70-1	69	41	194.17	MS, CR	0.18 ± 0.01^{a}	0.44 ± 0.03^{a}	1.87 ± 0.12^{a}	42.65 ± 10.90^{b}
3	*α*-2-propenyl-benzenmethanol	–	1244	936–58-3	107	79	148.09	MS	26.79 ± 0.02^{ab}	26.48 ± 0.61^{a}	26.59 ± 0.50^{a}	28.18 ± 1.25^{b}
4	pentamethylbenzene	1261	1260	700–12-9	133	148	148.13	MS, CR	0.00 ± 0.00^{a}	8.69 ± 0.54^{b}	20.64 ± 0.73^{c}	94.09 ± 3.17^{d}
5	*β*-terpenyl acetate	1272	1317	10198–23-9	93	68	196.15	MS, CR	0.00 ± 0.00^{a}	0.40 ± 0.07^{a}	13.21 ± 0.16^{b}	31.57 ± 6.24^{c}
6	(*E*, *E*)-2,4-decadienal	1322	1317	25152–84-5	81	41	152.12	MS, CR	0.00 ± 0.00^{a}	1.27 ± 0.13^{a}	82.26 ± 0.64^{b}	225.54 ± 49.86^{c}
7	verbenone	1228	1228	18309–32-5	107	91	150.10	MS, CR	0.00 ± 0.00^{a}	9.19 ± 0.63^{b}	31.09 ± 1.56^{c}	130.01 ± 8.70^{d}
8	*α*-muurolene	1499	1499	10208–80-7	105	161	204.19	MS, CR	8.83 ± 0.35^{a}	9.95 ± 0.98^{a}	11.18 ± 1.23^{a}	19.57 ± 5.26^{b}
9	*o*-xylorcinol	–	1490	527–55-9	138	123	138.07	MS	12.19 ± 0.52^{a}	13.33 ± 1.68^{a}	16.78 ± 2.61^{a}	33.55 ± 8.76^{b}
10	(*E*)-6-nonenal	–	1124	2277–20-5	41	55	140.12	MS	0.00 ± 0.00^{a}	12.38 ± 1.11^{a}	30.23 ± 6.66^{a}	229.18 ± 41.60^{b}
11	(*Z*)-3-nonen-1-ol	1156	1156	10340–23-5	55	68	142.14	MS, CR	0.00 ± 0.00 ^{a}	7.04 ± 0.52^{b}	14.64 ± 0.33^{c}	58.62 ± 3.11^{d}
12	7-methyl-3-methyleneoct-6-enal	1147	1147	55050–40-3	69	41	152.12	MS, CR	0.00 ± 0.00^{a}	5.45 ± 0.22^{b}	11.43 ± 0.12^{c}	49.21 ± 3.33^{d}
13	3-ethyl-3-methyldecane	–	1229	17312–66-2	57	85	184.22	MS	0.00 ± 0.00 ^{a}	0.39 ± 0.06^{ab}	1.56 ± 0.03^{b}	9.47 ± 1.27^{c}
14	*o*-*sec*-butylphenol	1252	1289	89–72-5	121	150	150.10	MS, CR	0.00 ± 0.00^{a}	4.71 ± 0.24^{b}	9.09 ± 0.59^{c}	38.56 ± 2.87^{d}
15	chavicol	1258	1255	501–92-8	134	133	134.07	MS, CR	0.00 ± 0.00^{a}	1.00 ± 0.05^{b}	2.47 ± 0.07^{c}	10.66 ± 0.88^{d}
16	(*Z*)-2-decenal	1250	1252	2497–25-8	41	55	154.14	MS, CR	0.00 ± 0.00^{a}	1.23 ± 0.10^{a}	3.09 ± 0.05^{b}	14.22 ± 1.44^{c}
17	(*E*)-2-dodecenal	1468	1468	20407–84-5	41	70	182.17	MS, CR	0.00 ± 0.00^{a}	0.15 ± 0.04^{a}	0.68 ± 0.08^{a}	16.27 ± 3.90^{b}
18	3,4-dimethyl-2,4,6-octatriene	1132	1121	57396–75-5	121	136	136.13	MS, CR	0.00 ± 0.00^{a}	3.21 ± 0.20^{a}	8.00 ± 1.76^{a}	62.18 ± 11.78^{b}
19	citronellal	1153	1153	106–23-0	154	95	154.14	MS, CR	0.00 ± 0.00^{a}	20.30 ± 1.03^{b}	42.48 ± 1.03^{c}	173.31 ± 10.33^{d}
20	*γ*-muurolene	1477	1477	30021–74-0	161	105	204.19	MS, CR	3.59 ± 0.30^{a}	3.99 ± 0.13^{a}	4.28 ± 0.24^{a}	6.99 ± 1.94^{b}
21	(3*E*)-3-nonen-1-ol	1143	1143	10339–61-4	55	41	142.14	MS, CR	0.00 ± 0.00^{a}	7.03 ± 0.42^{b}	14.63 ± 0.32^{c}	59.13 ± 3.60^{d}
22	hexyl-2-methylbutanoate	1236	1236	10032–15-2	103	57	186.16	MS, CR	0.00 ± 0.00^{a}	1.24 ± 0.05^{b}	3.94 ± 0.18^{c}	16.31 ± 1.11^{d}
23	methyl geranate	1326	1323	2349–14-6	69	41	182.13	MS, CR	0.00 ± 0.00^{a}	6.86 ± 0.63^{a}	345.52 ± 1.17^{b}	956.79 ± 186.85^{c}
24	(*E*)-carvone	1243	1242	99–49-0	82	54	150.10	MS, CR	11.57 ± 0.06^{a}	11.46 ± 0.12^{a}	11.51 ± 0.42^{a}	11.90 ± 0.34^{a}
25	4-vinylguaiacol	1312	1316	7786–61-0	135	150	150.07	MS, CR	0.00 ± 0.00^{a}	0.28 ± 0.04^{a}	11.56 ± 0.23^{b}	31.78 ± 6.71^{c}
26	4-pentenyl propionate	978	974	30563–30-5	57	68	142.10	MS, CR	8.91 ± 4.09^{a}	29.08 ± 4.21^{b}	95.06 ± 14.27^{c}	23.90 ± 1.62^{b}
27	4, 8-dimethyl-1, 3, 7-nonadiene	1117	1116	19945–61-0	69	41	150.14	MS, CR	0.00 ± 0.00^{a}	43.28 ± 3.86^{a}	106.24 ± 24.24^{a}	824.59 ± 155.89^{b}
28	isoxylaldehyde	1208	1208	5779–94-2	134	133	134.07	MS, CR	0.00 ± 0.00^{a}	0.64 ± 0.03^{ab}	2.38 ± 0.08^{b}	12.50 ± 1.90^{c}
29	piperitone oxide	1259	1256	5286–38-4	69	55	168.12	MS, CR	0.00 ± 0.00^{a}	2.20 ± 0.11^{b}	5.29 ± 0.09^{c}	24.11 ± 1.25^{d}
30	bornyl formate	1220	1226	7492–41-3	95	121	182.13	MS, CR	0.00 ± 0.00^{a}	2.80 ± 0.31^{ab}	11.39 ± 0.38^{b}	74.67 ± 10.29^{c}
31	3-formylphenol	1267	1327	100–83-4	122	121	122.04	MS, CR	0.00 ± 0.00^{a}	0.25 ± 0.04^{a}	7.01 ± 0.24^{b}	17.43 ± 3.54^{c}
32	*α*-zingiberene	1495	1495	495–60-3	119	93	204.19	MS, CR	9.18 ± 0.20^{a}	10.05 ± 1.12^{a}	11.60 ± 1.35^{a}	20.86 ± 5.60^{b}
33	*α*-cyclocitral	1116	1116	432–24-6	81	123	152.12	MS, CR	0.00 ± 0.00^{a}	9.28 ± 0.69^{a}	22.70 ± 5.23^{a}	180.25 ± 34.07^{b}
34	*o*-methylnitrobenzene	1155	1161	88–72-2	120	65	137.05	MS, CR	0.00 ± 0.00^{a}	5.11 ± 0.32^{b}	10.71 ± 0.19^{c}	47.26 ± 3.52^{d}
35	*trans*-chrysanthenyl acetate	1238	1239	50764–55-1	119	134	194.13	MS, CR	0.00 ± 0.00^{a}	2.33 ± 0.12^{b}	7.87 ± 0.46^{c}	33.56 ± 2.11^{d}
36	perillyl alcohol	–	1312	18457–55-1	68	79	152.12	MS	0.00 ± 0.00^{a}	0.60 ± 0.04^{a}	32.18 ± 0.20^{b}	87.16 ± 17.30^{c}

(*continued on next page*)

Table 1 (*continued*)

NO.	Compounds	Identification of the volatile components							Relative contents (μg/mL)			
		RRI	RI	CAS	Q1	Q2	M (Da)	IB	ZP	PI	PII	PIII
37	α-terpinen-7-al	1282	1283	1197–15-5	79	107	150.10	MS, CR	0.00 ± 0.00^{a}	166.88 ± 9.00^{b}	316.35 ± 18.80^{c}	1217.01 ± 73.75^{d}
38	propyl benzeneacetate	1331	1331	4606–15-9	91	92	178.10	MS, CR	0.00 ± 0.00^{a}	0.23 ± 0.02^{a}	14.38 ± 0.05^{b}	34.98 ± 6.51^{c}
39	α-caryophyllene	1451	1454	6753–98-6	93	80	204.19	MS, CR	0.30 ± 0.02^{a}	0.46 ± 0.05^{a}	0.97 ± 0.10^{a}	15.19 ± 3.94^{b}
40	butylbenzene	1053	1054	104–51-8	91	92	134.11	MS, CR	0.00 ± 0.00^{a}	9.67 ± 1.48^{a}	9.46 ± 1.06^{a}	433.33 ± 39.38^{b}
41	geranyl nitrile	–	1231	31983–27-4	69	41	149.12	MS	0.00 ± 0.00^{a}	2.20 ± 0.08^{a}	8.23 ± 0.23^{b}	45.85 ± 5.01^{c}
42	linalyl acetate	1256	1257	115–95-7	93	80	196.15	MS, CR	0.00 ± 0.00^{a}	2.12 ± 0.13^{b}	4.64 ± 0.16^{c}	21.56 ± 1.88^{d}
43	decanol	1272	1272	112–30-1	70	55	158.17	MS, CR	0.00 ± 0.00^{a}	4.30 ± 0.23^{b}	8.51 ± 0.52^{c}	33.27 ± 1.90^{d}
44	2, 4-decadienol	1295	1274	14507–02-9	41	55	154.14	MS, CR	0.00 ± 0.00^{a}	127.52 ± 6.97^{b}	268.70 ± 12.11^{c}	1216.42 ± 100.20^{d}
45	2-cyano-2-ethyl-butyramide	–	1287	18705–38-9	82	97	140.10	MS	0.00 ± 0.00^{a}	434.70 ± 28.65^{a}	1040.56 ± 36.81^{b}	6154.87 ± 640.47^{c}
46	car-3-en-5-one	1314	1314	81800–50-2	107	150	150.10	MS, CR	0.00 ± 0.00^{a}	0.90 ± 0.10^{a}	35.78 ± 0.82^{b}	94.95 ± 19.74^{c}
47	phenol	981	980	108–95-2	94	66	94.04	MS, CR	5.01 ± 0.22^{a}	6.51 ± 0.33^{a}	11.65 ± 1.81^{b}	17.98 ± 0.36^{c}
48	adamantane	1117	1116	281–23-2	136	79	136.13	MS, CR	0.00 ± 0.00^{a}	1.00 ± 0.09^{a}	2.33 ± 0.53^{a}	17.94 ± 3.27^{b}
49	cinnamaldehyde	1278	1274	104–55-2	131	132	132.06	MS, CR	0.00 ± 0.00^{a}	4.76 ± 0.22^{ab}	10.72 ± 0.28^{b}	65.12 ± 7.58^{c}
50	panaxene	1314	1314	871660–95-6	121	105	204.19	MS, CR	0.00 ± 0.00^{a}	0.33 ± 0.02^{a}	9.09 ± 0.18^{b}	23.93 ± 5.00^{c}
51	*p*-hydroxyacetophenone	1442	1455	99–93-4	121	136	136.05	MS, CR	0.00 ± 0.00^{a}	0.14 ± 0.02^{a}	0.38 ± 0.03^{a}	9.60 ± 2.49^{b}
52	isopropyl benzoate	1223	1217	939–48-0	105	77	164.08	MS, CR	0.00 ± 0.00^{a}	12.93 ± 0.83^{b}	43.89 ± 1.96^{c}	190.55 ± 12.82^{d}
53	veratrol	1147	1148	91–16-7	138	95	138.07	MS, CR	0.00 ± 0.00^{a}	3.69 ± 0.22^{b}	14.43 ± 1.90^{c}	33.85 ± 0.57^{d}
54	*trans*-limonene oxide	1139	1139	6909–30-4	94	108	152.12	MS, CR	0.00 ± 0.00^{a}	12.65 ± 0.70^{b}	26.49 ± 0.57^{c}	115.45 ± 7.05^{d}
55	*p*-acetylethylbenzene	1274	1277	937–30-4	133	148	148.09	MS, CR	0.00 ± 0.00^{a}	159.26 ± 12.03^{b}	292.87 ± 19.26^{c}	823.65 ± 47.62^{d}
56	dihydromethyl cinnamate	1279	1279	103–25-3	104	91	164.08	MS, CR	0.00 ± 0.00^{a}	13.19 ± 0.76^{b}	22.17 ± 1.58^{c}	67.79 ± 3.35^{d}
57	*p*-vinylanisole	1155	1156	637–69-4	134	91	134.07	MS, CR	0.00 ± 0.00^{a}	6.65 ± 0.34^{b}	14.17 ± 0.40^{c}	64.95 ± 4.91^{d}
58	borneo camphor	1146	1145	76–22-2	95	41	152.12	MS, CR	0.00 ± 0.00^{a}	1.73 ± 0.11^{b}	5.23 ± 0.48^{c}	15.68 ± 0.70^{d}
59	*p*-hydroquinone	1241	1283	123–31-9	110	81	110.04	MS, CR	0.00 ± 0.00^{a}	1.43 ± 0.12^{b}	2.67 ± 0.14^{c}	10.28 ± 0.80^{d}
60	*trans*-anethole	1281	1283	4180–23-8	148	147	148.09	MS, CR	0.00 ± 0.00^{a}	182.37 ± 12.71^{b}	330.10 ± 19.21^{c}	947.02 ± 63.83^{d}
61	*d*-camphor	1144	1144	464–49-3	95	81	152.12	MS, CR	0.00 ± 0.00^{a}	1.78 ± 0.12^{b}	5.24 ± 0.54^{c}	16.24 ± 0.40^{d}
62	2-ethylhexyl acetate	1144	1129	103–09-3	70	43	172.15	MS, CR	0.00 ± 0.00^{a}	2.55 ± 0.24^{a}	6.36 ± 1.59^{a}	49.99 ± 9.59^{b}
63	(*E*)-myroxide	1143	1141	28977–57-3	79	81	152.12	MS, CR	0.00 ± 0.00^{a}	81.27 ± 4.47^{b}	168.96 ± 3.29^{c}	720.78 ± 46.07^{d}
64	4-methylpentyl-2-methylbutyrate	1201	1143	35852–40-5	103	57	186.16	MS, CR	0.00 ± 0.00^{a}	10.80 ± 0.66^{b}	22.26 ± 0.51^{c}	95.19 ± 5.84^{d}
65	camphenone	1149	1114	55659–42-2	93	108	150.10	MS, CR	0.00 ± 0.00^{a}	2.79 ± 0.15^{a}	7.22 ± 1.07^{a}	48.62 ± 7.87^{b}
66	nerol oxide	1151	1154	1786–08-9	68	67	152.12	MS, CR	0.00 ± 0.00^{a}	1.64 ± 0.13^{b}	3.49 ± 0.14^{c}	15.07 ± 0.96^{d}
67	2-oxocineole	1217	1217	107598–08-3	82	43	168.12	MS, CR	0.00 ± 0.00^{a}	0.90 ± 0.08^{a}	3.74 ± 0.15^{b}	21.85 ± 2.54^{c}
68	*trans*-carveole	1219	1217	1197–07-5	109	84	152.12	MS, CR	0.00 ± 0.00^{a}	2.45 ± 0.17^{ab}	10.38 ± 0.13^{b}	68.87 ± 10.15^{c}
69	8, 9-dehydrothymol	1221	1221	18612–99-2	148	105	148.09	MS, CR	0.00 ± 0.00^{a}	6.82 ± 0.43^{b}	23.25 ± 1.13^{c}	90.84 ± 4.42^{d}
70	cumaldehyde	1236	1239	122–03-2	133	105	148.09	MS, CR	0.00 ± 0.00^{a}	7.79 ± 0.49^{b}	27.09 ± 1.29^{c}	117.59 ± 8.12^{d}
71	5-methyl-5-propylnonane	–	1229	17312–75-3	71	57	184.22	MS	0.00 ± 0.00^{a}	1.51 ± 0.07^{ab}	6.27 ± 0.12^{b}	40.94 ± 5.59^{c}
72	anisole	916	921	100–66-3	108	78	108.06	MS, CR	0.00 ± 0.00^{a}	2.65 ± 0.14^{b}	2.03 ± 0.06^{b}	9.56 ± 0.64^{c}
73	benzoic aldehyde	961	960	100–52-7	77	106	106.04	MS, CR	1.78 ± 0.19^{a}	2.26 ± 0.28^{a}	1.03 ± 0.29^{a}	33.67 ± 2.34^{b}

(*continued on next page*)

Table 1 (*continued*)

NO.	Compounds	Identification of the volatile components							Relative contents (μg/mL)			
		RRI	RI	CAS	Q1	Q2	M (Da)	IB	ZP	PI	PII	PIII
74	albene	1167	1159	38451–64-8	95	94	162.14	MS, CR	0.00 ± 0.00^{a}	1.77 ± 0.14^{b}	5.16 ± 0.53^{c}	16.01 ± 0.42^{d}
75	*β*-ocimene	1037	1037	13877–91-3	93	91	136.13	MS, CR	0.00 ± 0.00^{a}	0.16 ± 0.03^{a}	0.14 ± 0.02^{a}	7.38 ± 0.62^{b}
76	durene	1108	1115	95–93-2	119	134	134.11	MS, CR	0.00 ± 0.00^{a}	0.56 ± 0.04^{a}	1.17 ± 0.19^{a}	7.70 ± 1.28^{b}
77	*β*-linalool	1101	1099	78–70-6	71	93	154.14	MS, CR	4.06 ± 0.33^{a}	3.83 ± 0.03^{ab}	4.24 ± 0.12^{b}	5.76 ± 0.22^{c}
78	filifolone	1108	1108	4613–37-0	80	79	150.10	MS, CR	0.00 ± 0.00^{a}	1.71 ± 0.13^{a}	4.01 ± 0.77^{a}	30.03 ± 5.39^{b}
79	2-furanacrolein	1111	1111	623–30-3	65	122	122.04	MS, CR	0.00 ± 0.00^{a}	1.65 ± 0.05^{a}	5.26 ± 0.59^{a}	34.67 ± 5.92^{b}
80	*p*-tolyl-acetaldehyde	1120	1120	104–09-6	105	77	134.07	MS, CR	0.00 ± 0.00^{a}	1.48 ± 0.14^{ab}	3.51 ± 0.40^{b}	22.15 ± 3.42^{c}
81	chrysanthenone	1121	1123	473–06-3	107	91	150.10	MS, CR	0.00 ± 0.00^{a}	7.68 ± 0.58^{a}	18.80 ± 4.07^{a}	142.57 ± 25.63^{b}
82	allo- neoocimene	1144	1144	3016–19-1	121	79	136.13	MS, CR	0.00 ± 0.00^{a}	1.16 ± 0.09^{b}	2.49 ± 0.01^{c}	10.39 ± 0.78^{d}
83	*α*-phenylacrolein	1152	1152	4432–63-7	103	77	132.06	MS, CR	0.00 ± 0.00^{a}	10.72 ± 0.51^{b}	22.39 ± 0.52^{c}	95.61 ± 5.92^{d}
84	tetralin	1155	1155	3	104	132	132.09	MS, CR	0.00 ± 0.00^{a}	6.83 ± 0.45^{b}	13.76 ± 0.43^{c}	59.76 ± 3.19^{d}
85	phellandral	1273	1276	21391–98-0	109	41	152.12	MS, CR	0.00 ± 0.00^{a}	7.19 ± 0.28^{b}	14.51 ± 0.91^{c}	55.12 ± 3.25^{d}
86	3-*o*-tolylpentane	1239	1240	54410–74-1	105	133	162.14	MS, CR	0.53 ± 0.02^{a}	1.13 ± 0.08^{ab}	1.99 ± 0.15^{b}	10.14 ± 1.00^{c}
87	allyl benzoate	1254	1254	583–04-0	105	77	162.07	MS, CR	0.00 ± 0.00^{a}	9.40 ± 0.90^{b}	22.40 ± 1.14^{c}	94.13 ± 6.00^{d}
88	*cis*-anethole	1252	1254	25679–28-1	148	147	148.09	MS, CR	0.00 ± 0.00^{a}	11.93 ± 0.92^{a}	28.35 ± 0.93^{b}	132.96 ± 12.89^{c}
89	perilla aldehyde	1276	1274	2111–75-3	68	79	150.10	MS, CR	0.00 ± 0.00^{a}	16.95 ± 0.97^{b}	37.37 ± 1.45^{c}	186.45 ± 15.88^{d}
90	5-undecanol	1376	1288	37493–70-2	69	55	172.18	MS, CR	0.00 ± 0.00^{a}	43.46 ± 2.99^{b}	80.38 ± 4.97^{c}	278.38 ± 15.47^{d}
91	2-phenylcrotonaldehyde	1274	1276	4411–89-6	117	146	146.07	MS, CR	0.00 ± 0.00^{a}	47.55 ± 3.01^{b}	81.40 ± 6.01^{c}	248.65 ± 12.74^{d}
92	6-undecanol	1281	1277	23708–56-7	83	55	172.18	MS, CR	0.00 ± 0.00^{a}	358.67 ± 17.99^{b}	592.02 ± 24.48^{c}	1822.92 ± 151.10 ^{d}
93	2-hexylpyridine	–	1284	1129–69-7	93	106	163.14	MS	0.00 ± 0.00^{a}	146.21 ± 7.04^{b}	258.97 ± 17.84^{c}	806.51 ± 35.95^{d}
94	terephthaladehyde	1166	1284	623–27-8	134	133	134.04	MS, CR	0.00 ± 0.00^{a}	19.52 ± 0.86^{b}	35.74 ± 2.48^{c}	104.11 ± 5.71^{d}
95	camphoroquinone	–	1319	10373–78-1	95	69	166.10	MS	0.00 ± 0.00^{a}	0.20 ± 0.02^{a}	11.37 ± 0.13^{b}	30.11 ± 5.91^{c}
96	isobutyl benzoate	1331	1321	120–50-3	105	123	178.10	MS, CR	0.00 ± 0.00^{a}	0.24 ± 0.02^{a}	6.84 ± 0.19^{b}	16.85 ± 3.06^{c}
97	nerolic acid	1347	1344	4613–38-1	69	41	168.12	MS, CR	0.00 ± 0.00^{a}	0.00 ± 0.00^{a}	0.00 ± 0.00^{a}	23.31 ± 5.60^{b}
98	(*E*, *Z*)-3,6-nonadienol	1156	1156	56805–23-3	67	93	140.12	MS, CR	0.00 ± 0.00^{a}	10.31 ± 0.67^{b}	21.41 ± 0.44^{c}	88.58 ± 4.98^{d}
99	eremophilene	1486	1494	10219–75-7	107	161	204.19	MS, CR	8.72 ± 0.24^{a}	9.74 ± 0.92^{a}	10.95 ± 1.17^{a}	19.62 ± 5.43^{b}
100	guaiacol	1090	1089	90–05-1	109	124	124.05	MS, CR	0.00 ± 0.00^{a}	13.04 ± 0.64^{b}	20.66 ± 2.82^{c}	82.97 ± 1.54^{d}
101	dipropyl disulfide	1098	1107	629–19-6	150	108	150.05	MS, CR	0.00 ± 0.00^{a}	7.55 ± 0.62^{a}	18.72 ± 4.33^{a}	151.14 ± 29.10^{b}
102	furfuryl methyl disulfide	1226	1226	57500–00-2	81	53	160.00	MS, CR	0.00 ± 0.00^{a}	3.00 ± 0.20^{a}	11.47 ± 0.40^{b}	65.91 ± 7.94^{c}

DVB/CWR/PDMS fiber at the same temperature for 15 min.

GC–MS analysis

The volatile compounds were separated on a DB-5MS column (30 m × 0.25 mm × 0.25 μm film thickness; Agilent J&W Scientific, Folsom, CA, USA) at splitless mode installed on an Agilent 8890 gas chromatograph equipped with a Agilent 7000D mass spectrometer (Santa Clara, CA, USA). The GC–MS system was controlled and operated using an Agilent Mass-hunter. Helium (99.999 %) was selected as the carrier gas at a linear velocity of 1.2 mL/min. The temperatures of 250 °C were set for the injector. To ensure the complete desorption of volatile components, the SPME fiber need to be inserted into the heated GC injector after sampling and maintained at 250 °C for 5 min. The temperature program of column was set as follows: first, the initial column temperature was maintained at 40 °C for 3.5 min, followed by a ramp of 10 °C/min to 100 °C, then a ramp of 7 °C/min to 180 °C, finally increased to 280 °C at a rate of 25 °C/min, and held at 280 °C for 5 min. For MS, selected ion monitoring (SIM) mode was used for the identification and quantification of analytes. The ionization voltage was 70 eV, and the temperatures of ion source, quadrupole mass detector and transfer line were 230, 150 and 280 °C, respectively. The total ionic chromatogram (TIC) with *m/z* range of 50–450 was obtained (Supplementary Fig. 1).

Identification and quantification of volatile components

In this study, Agilent MassHunter software was used for the initial processing and analysis of raw mass spectrometry data. Automated mass spectral deconvolution and identification system (AMDIS) software was used to achieve chromatographic peak deconvolution (Huang et al., 2022). Volatile compounds in the stipe of *Phallus impudicus* during the growth period were identified by comparing retention index (RI) and mass spectra with reference standards, literatures or NIST Chemistry WebBook (https://webbook.nist.gov/chemistry and NIST 2020). Of them, the literature RI values were obtained from the NIST database. In addition, for the mass spectrum of the sample after deducting the background, if the retention time detected was close to the standard reference, it was determined to be the substance (Yuan et al., 2022). The relevant indicators for the identification of each identified compound were shown in Table 1. The [3,4,5,6-2H4]-Methyl 2-hydroxybenzoate was used as an internal standard for semi-quantitative analysis of the identified volatile compounds. Assuming that C, C_{is}, Ac and A_{is} represent the relative content of analyte, the final content of internal standard in sample, the peak area of analyte and the peak area of internal standard, respectively, the relative content of analyte C can be calculated according to the formula below: $C = (Ac / A_{is}) \times C_{is}$ (Shen et al., 2023). The relative contents of volatile compounds were expressed as μg/mL, and three biological replicates were conducted for all samples.

Statistical analysis

All data were analyzed statistically using IBM SPSS Statistics 22.0, and graphic production was conducted using GraphPad Prism 7 and Photoshop 6.0. Principal component analysis (PCA) was completed with the help of R Software (R i386 ver. 3.3.3). The relative quantitative values were presented as mean ± standard deviation of three biological replicates. Duncan's multiple comparisons were used to analyze the spatiotemporal dynamic changes of volatile compounds in the stipe of *Phallus impudicus* during different growth stages. The OPLS-DA was carried out according to the reference of Thévenot et al. (2015). Metabolites satisfying the criteria for both variable importance in projection (VIP) > 1 and P value < 0.05 that obtained by the method of OPLS-DA and PLS-DA were differential metabolites. Correlation heatmap with signs was constructed with the R software package (R version 3.6.3), and the relationship between different developmental stages and the different volatile compounds were proved by Pearson correlation coefficient. $P < 0.05$ was recognized as statistical significance.

Result and discussion

Identification and quantitative descriptive analysis of volatile compounds

Regarding the Gómez et al. (2022) and Tagkouli et al. (2021) for the method of determining edible fungi, volatile compounds in the stipe of *Phallus impudicus* at four different developmental stages were measured by headspace solid-phase microextraction coupled with gas chromatography-mass spectrometry (HS-SPME-GC–MS). The identification information of all the volatile compounds was summarized in Table 1, 102 metabolites were identified successfully based on the MS information and RI. Obviously, the identified compounds in samples showed the same change tendency during the whole developmental period, that was, the metabolites accumulated continuously over time. For most of the volatile compounds found in the stipe of *Phallus impudicus*, there were significant differences in the relative content of the four different developmental stages, especially for the latter three stages. The volatile compounds with the highest relative content were 2-cyano-2-ethyl-butyramide and 6-undecanol, followed by α-terpinen-7-al, 2, 4-decadienol and methyl geranate, from shell breaking stage to mature stage, ranging from 434.70 to 6154.87, 358.67–1822.92, 166.88–1217.01, 127.52–1216.42 and 6.86–956.79, respectively. Of them, the 2-cyano-2-ethyl-butyramide had not been reported in other edible fungi, which might be the characteristic volatile component of *Phallus impudicus*. In addition, *trans*-anethole, *p*-acetylethylbenzene, 2-hexylpyridine, (*E*)-myroxide, (*E*, *E*)-2,4-decadienal, verbenone, (*E*)-6-nonenal, citronellal, 4, 8-dimethyl-1, 3, 7-nonadiene, *α*-cyclocitral, butylbenzene, isopropyl benzoate, chrysanthenone, *cis*-anethole, perilla aldehyde, 5-undecanol and 2-phenylcrotonaldehyde with relative content range of 1.27–947.02 were also key contributors to the volatile composition and flavor formation of *Phallus impudicus*. The lowest relative volatile component content observed in the stipe of *Phallus impudicus* at the latter three stages was *β*-linalool and *γ*-muurolene, followed by *β*-ocimene, durene, 3-ethyl-3-methyldecane, anisole and *p*-hydroxyacetophenone, ranging from 3.83 to 5.76, 3.99–6.99, 0.16–7.38, 0.56–7.70, 0.39–9.47, 2.65–9.56 and 0.14–9.60, respectively. According to the semi-quantitative results obtained, except for a small amount of accumulation of 14 metabolites (eremophilene, 3-*o*-tolylpentane, *β*-linalool, benzoic aldehyde, phenol, *α*-caryophyllene,*α*-zingiberene, 4-pentenyl propionate, (*E*)-carvone, *γ*-muurolene, *α*-muurolene, *o*-xylorcinol, geranylacetone and *α*-2-propenyl-benzenmethanol) at the budding stage, the remaining 88 metabolites were not detected at this stage, which indicated that the production, accumulation and release of volatile compounds mainly occurred after the shell was broken by the thallus of mushroom. The dimethyl oligosulfides (including dimethyl disulfide, dimethyl trisulfide) were the main reason for the special flavor of ripe body (Gupta, Jayaprakash & Shinde, 2016; Pudil, Uvira & Janda, 2014). It is worth mentioning that the sulfide did not form at ZP stage in this study, and the sulfide increased significantly until the mature stage of PIII, which was consistent with the characterization results of Pudil, Uvira and Janda (2014) in identified sulfide from the *Phallus impudicus* L. Ex Pers at mature stage. Taken together, these findings indicated that adequate growth can improve the overall content of volatile compounds in the stipe of *Phallus impudicus*, which largely determined the quality and nutritional value of this regional characteristic edible fungus. Furthermore, the types and concentrations of volatile compounds in the edible mushroom of *Phallus impudicus* were mainly dependent on the growth stage, which was consistent with the research results of Cho, Seo and Kim (2003) and Feng et al. (2021).

Analysis profiles of volatile compounds

Existing studies have shown that 3 % of volatile compounds had odor activity, which had the greatest impact on the overall aroma or flavor of food (Dunkel et al., 2014). *Phallus impudicus* had a special odor and unique flavor, which was related to the complex mixture of compounds belonging to the different chemical categories. In this study, 102 volatile compounds were identified from the stipe of *Phallus impudicus* by SPME-GC–MS, which has been described in section 3.1. The data thus obtained were subjected to further analysis. Fig. 2A showed that 13 of the 102 volatile compounds were common in samples at four developmental stages. According to their different types, the identified 102 volatile compounds can be divided into nitrogen compounds, ether, hydrocarbons, phenol, heterocyclic compounds, ketone, ester, aromatics, aldehyde, terpenoids, alcohol and amine. Among them, amine, alcohol, aldehyde and terpenoids were the main components of aroma, and the total content of those four compounds accounted for about 70.47 % of the total volatile compounds at PIII stage (Fig. 2B). To further analyze the effect of growth stage on the aroma of *Phallus impudicus* fruit-body, multivariate statistical analysis was performed on 102 volatile compounds obtained qualitatively and semi-quantitatively, as shown in Fig. 2. In view of the complexity of the data, principal component analysis (PCA) was used to display the distribution and variation of data points visually and intuitively (Granato, Santos, Escher, Ferreira & Maggio, 2018). It can be clearly seen from Fig. 2C that the volatile compounds changed significantly during the whole growth process. The PCA score plot (13 samples, 102 volatile compounds) indicated that the *Phallus impudicus* at different growth stages can be well separated by the

first two principal components, and the first two components could account for 97.52 % of the total variability, of which PC1 explained 95.49 % and PC2 explained 2.07 % (Fig. 2C). In addition, the samples can be intuitively divided into different groups or clusters by hierarchical cluster analysis (HCA). As shown in Fig. 2D, a total of 13 samples from four stages were classified into three categories by hierarchical cluster analysis, among which ZP and PI were one category, PII and PIII were one category respectively. Based on the results of PCA and HCA, it was speculated that the *Phallus impudicus* underwent a dramatic change in aroma quality at the rapid growth stage (PII) and mature stage (PIII).

OPLS-DA results

OPLS-DA can be used to filter out the orthogonal variables that are not related to the categorical variables in the metabolites, and the analysis of non-orthogonal variables and orthogonal variables can be carried out without interference to each other, so as to obtain the intergroup differences of metabolites with high reliability and the correlation degree information of experimental groups (Bao, Mu & Wang, 2023). The Fig. 3A showed the OPLS-DA score diagram of the four different developmental stages of *Phallus impudicus*. As shown in Fig. 3A, the 12 samples were all within the confidence intervals, and the four stages of samples were well distinguished, and the differences between the groups were significant. The above information indicated that the growth stage had a significant effect on the volatile metabolites of *Phallus impudicus*. In addition, there was no overlap between the samples, and the separation degree was high. The clustering of samples in the budding stage, the shell breaking stage and the rapid growth stage was strong, but the clustering of samples at the mature stage was poor. This might be because although the volatile components of these samples at mature stage were highly similar, the degree of accumulation varied greatly, and the influence of internal and external factors on different growth stages was different. The permutation test results of the OPLS-DA model were presented in Fig. 3B, and each group of models had two principal components (PCs). The cumulative values of R^2X, R^2Y and Q^2 were equal to 0.985, 0.994 and 0.96, respectively. The S-plot of OPLS-DA presented multiple metabolites as shown Fig. 3C. Obviously, the permutation test results demonstrated that the OPLS-DA model was realistic and reliable, and there was no over-fitting phenomenon.

Identification of differential metabolites

In this study, the statistical method PLS-DA was used for supervised discriminant analysis. The VIP value was obtained to evaluate the strength and explanatory power of the expression pattern of each metabolite on the categorical discrimination of each group of samples, so as to effectively screen for biologically significant differential metabolites, also known as marker metabolites (Li, Zuo & Wang, 2022). The greater the VIP value of the metabolite, the greater the decisive effect on the sample discrimination. The VIP values of the first two principal components obtained by OPLS-DA model were applied to the screening of marker metabolites. As shown in Table S1 and Fig. 4, the top 50 differential metabolites with the highest VIP value were screened out from the four different developmental stages based on VIP > 1 and $P < 0.05$, which mainly included alcohol, aldehyde, ether, ketone, phenol, and other secondary metabolites. This result was agreed with Feng et al. (2021) that the differential volatile metabolites in edible fungi of *Agaricus bisporus* at growth stages were mainly composed of alcohols, aldehydes, ketones, etc. Specifically, the 50 differential metabolites screened included 1 amine (2-cyano-2-ethyl-butyramide), 7 alcohols (6-undecanol, 5-undecanol, 2, 4-decadienol, (E, Z)-3,6-nonadienol, (Z)-3-nonen-1-ol, (3E)-3-nonen-1-ol and decanol), 8 aromatics (*trans*-anethole, anisole, α-phenylacrolein, tetralin, p-vinylanisole, o-methylnitrobenzene, pentamethylbenzene and veratrol), 4 phenols (guaiacol, o-*sec*-butylphenol, p-hydroquinone and 8, 9-dehydrothymol), 1 ether (*cis*-anethole), 8 aldehydes (2-phenylcrotonaldehyde, α-terpinen-7-al, terephthaladehyde, perilla aldehyde, 7-methyl-3-methyleneoct-6-enal, cinnamaldehyde, (E)-6-nonenal and α-cyclocitral), 12 terpenoids ((E)-myroxide, citronellal, phellandral, (+)-*trans*-limonene oxide, 4, 8-dimethyl-1, 3, 7-nonadiene, verbenone, d-camphor, borneo camphor, cumaldehyde, nerol oxide, linalyl acetate and allo-neoocimene), 1

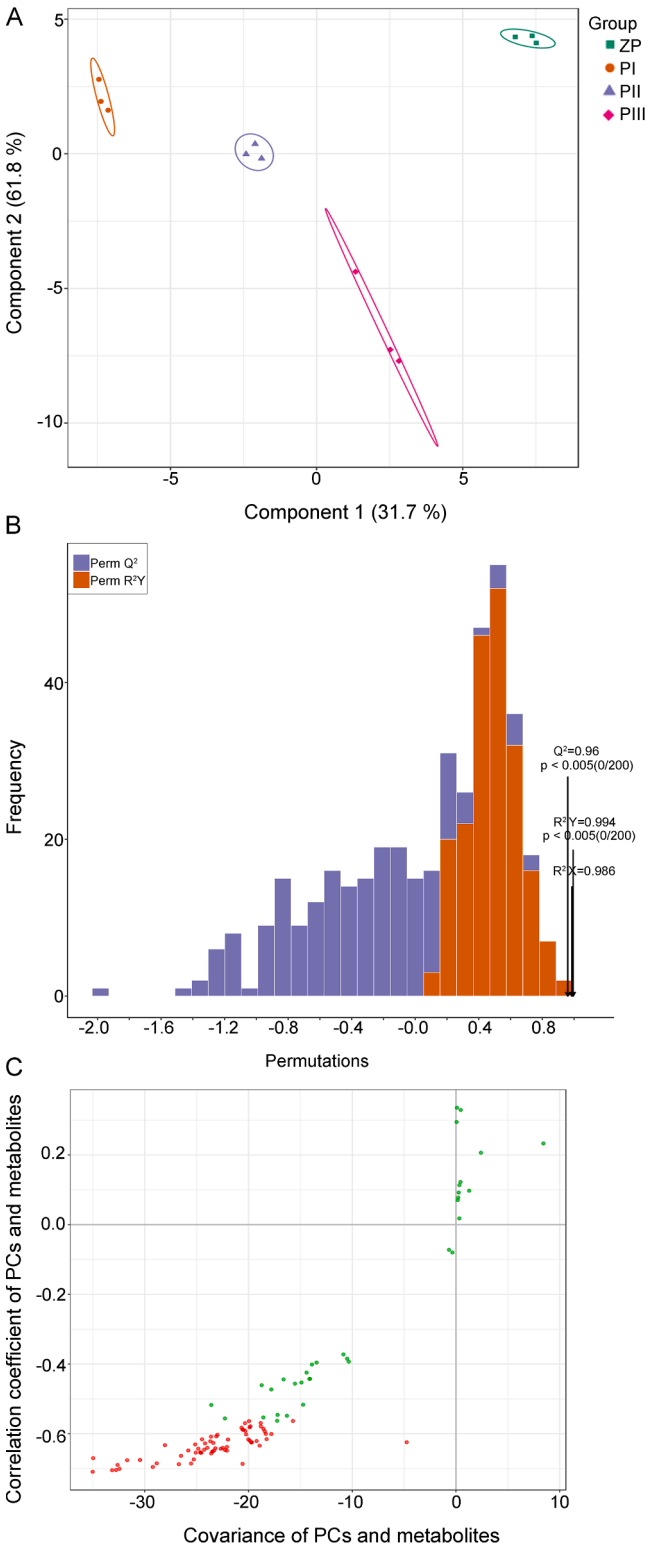

Fig. 3. The results of OPLS-DA. OPLS-DA, orthogonal partial least squares-discriminant analysis; PCs, principal components. (A) indicated the scores of OPLS-DA plot; (B) meant the model validation diagram of OPLS-DA; (C) indicated the S-plot of OPLS-DA.

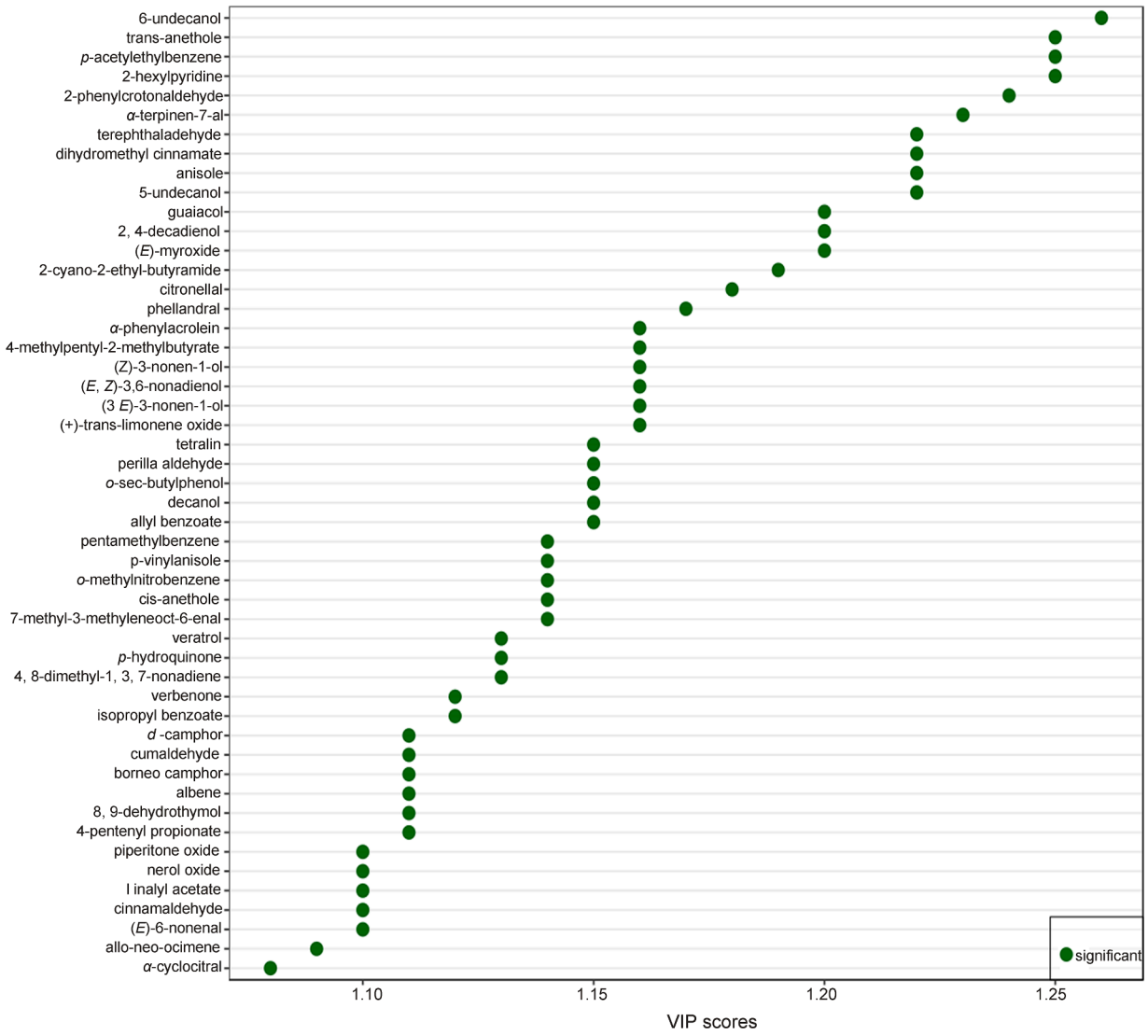

Fig. 4. The top 50 volatile metabolites of *Phallus impudicus* with the highest VIP value at different developmental stages obtain by the PLS-DA method. VIP, variable importance in projection; PLS-DA, partial least squares-discriminant analysis. Both the value of VIP > 1 and the $P < 0.05$ was considered as a significant difference.

hydrocarbon (albene), 2 ketones (p-acetylethylbenzene and piperitone oxide), 1 heterocyclic compound (2-hexylpyridine) and 5 esters (dihydromethyl cinnamate, 4-methylpentyl-2-methylbutyrate, allyl benzoate, isopropyl benzoate and 4-pentenyl propionate). According to the synthesis pathway of precursors, most of the above volatiles belonged to the category of isoprenoid-, amino acid- and fatty acid-derived volatile compounds, which were similar to the composition of volatile substances in plants (Dombrowski et al., 2019; Mostafa et al., 2022; Shen et al., 2023).

Correlation analysis of different stages and differential metabolites

In order to intuitively represent the correlation between different developmental stages and the change patterns of 50 differential metabolites at developmental stages, heatmap analysis was used in this study, and the results were shown in Fig. 5. From the Fig. 5A, it showed that the correlation coefficients of the latter three stages were all greater than 0.5, while the correlation between the first stage and the latter three stages was not strong. Obviously, the shell breaking of *Phallus impudicus* fruiting bodies was the promoter for the synthesis and accumulation of volatile compounds. It was worth noting that the contents of 50 volatile compounds all showed a significant upward trend throughout the growth period, and the maximum accumulation was all obtained at the maturity stage, except for 4-pentenyl propionate (the highest value at rapid growth stage) (Fig. 5B). In other words, among the 50 kinds of representative differential metabolites, a large amount of volatile compounds were absent or extremely low in all samples (the blue region of circus-heatmap, Fig. 5B), which demonstrated that the growth stages affected the synthesis and accumulation of volatile compounds. The concentration of key aroma compounds was the highest at mature stage and the lowest at the beginning of growth, which was contrary to the results of Feng et al. (2021) on the volatile profiles of *Agaricus bisporus* at different growth stages. Furthermore, the studies had identified 11 key aroma compounds in button mushroom, such as 2-octenal, 1-octen-3-one, (E)-2-octen-1-ol, etc., which were completely different from the main aroma compounds identified in this study (Feng et al., 2021; Sun, Zhang, Xin, Sun & Xu, 2020). The inconsistency of the results might be due to the different types of edible fungi or the different separation and determination methods of volatile compounds, but it also once again proved the uniqueness of the flavor of *Phallus impudicus*. Nevertheless, the conclusion that the change of key aroma mainly depended on the growth stage in this study was the same with the *Agaricus bisporus* (Feng et al., 2021), which also showed the importance of growth stage for the flavor formation in edible fungi.

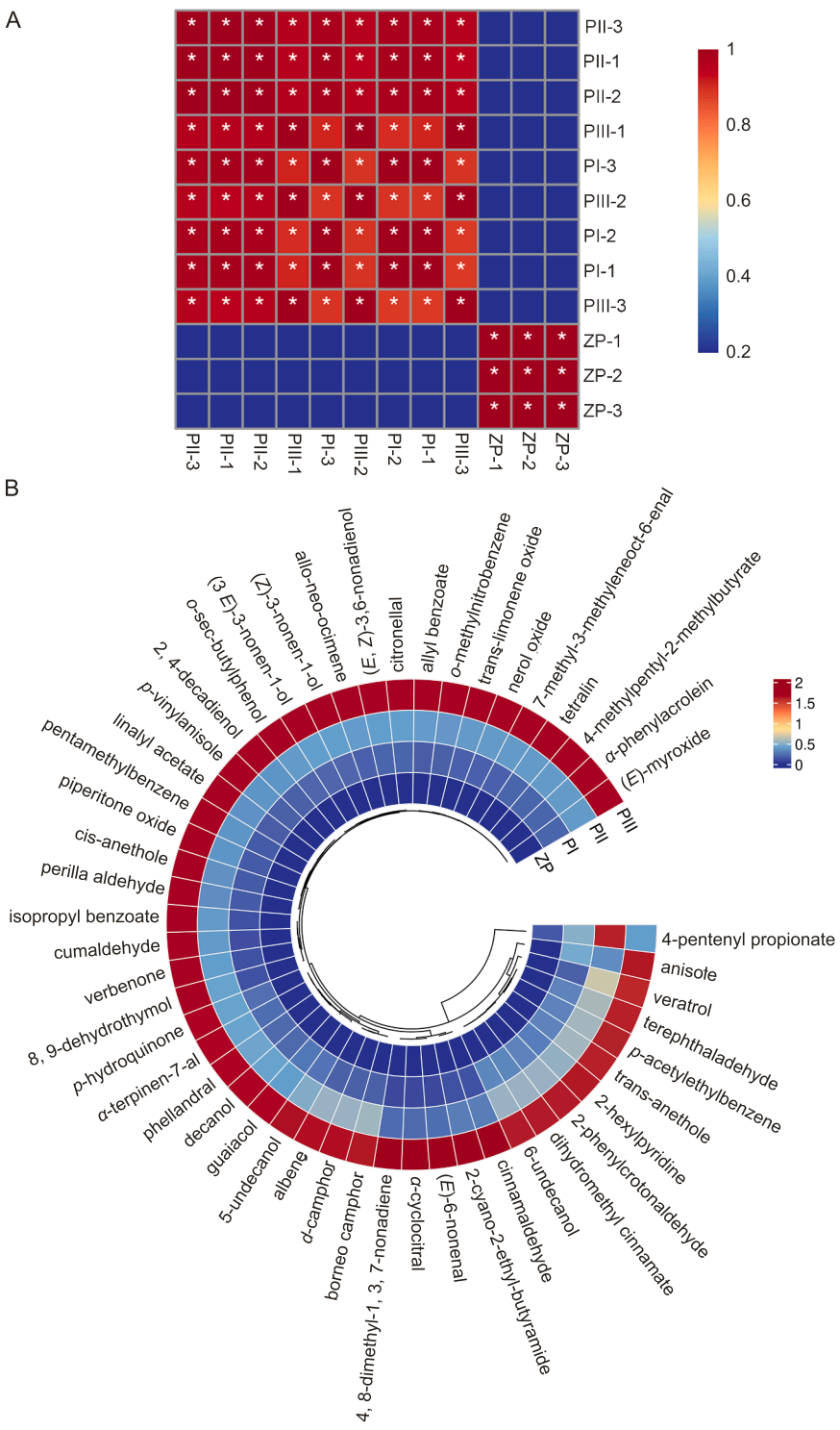

Fig. 5. The correlation analysis based on the top 50 volatile metabolites of *Phallus impudicus* with the highest VIP value. (A) indicated the correlation heatmap among the different development stage; (B) meant the circus-heatmap among the top 50 volatile metabolites of *Phallus impudicus* with the highest VIP value.

In order to further understand how the 50 volatile compounds with the highest VIP obtained by PLS-DA were coordinated during the development of *Phallus impudicus*, a correlation heatmap was constructed to investigate the potential relationships between these stage-dependent differential metabolites. Interestingly, as shown in Supplementary Fig. 2, except for 4-pentenyl propionate, the other 49 volatile compounds, including 1 amine, 7 alcohols, 8 aromatics, 4 phenols, 1 ether, 8 aldehydes, 12 terpenoids, 5 esters, 1 hydrocarbon, 2 ketones and 1 heterocyclic compound, were strongly correlated with each other, and the correlations between these metabolites tended to be significantly positive. There was no significant correlation between 4-pentenyl propionate and the other 49 differential metabolites, which corresponded to the different stage-dependent distribution characteristics of this compound compared to other compounds (as shown in Fig. 5B). In addition, among the top 5 compounds with relatively high content (Table 1), only 6-undecanol, α-terpinen-7-al, 2, 4-decadienol and 2-cyano-2-ethyl-butyramide with high VIP values were screened as differential metabolites (Fig. 5B), which indicated that the four volatile compounds above

might mainly contribute the flavor formation. The above information indicated that volatile compounds (mainly 6-undecanol, α-terpinen-7-al, 2, 4-decadienol and 2-cyano-2-ethyl-butyramide) might regulated the flavor formation of fruiting bodies in *Phallus impudicus* during the growth stage through the synergistic interaction with other volatiles. Moreover, the above results further confirmed that volatile compounds, a variety of secondary metabolites, were the main contributors to the unique flavor of edible fungi (Sun et al., 2022).

Conclusions

A total of 102 volatile compounds were identified from the fruiting bodies of *Phallus impudicus* after shell breaking. According to PC1 and PC2 in the PCA plot, they accounted for 95.49 % and 2.07 % of the total variance of volatile compounds, respectively. The volatile compounds in the stipes of *Phallus impudicus* at growth stages could be separated and exhibited significant differences. The differential volatile metabolites were obtained by the method of OPLS-DA and PLS-DA, among which the top 50 metabolites with the largest VIP value was clearly distinguished at the four different growth stages, especially from the rapid growth stage to the mature stage, where almost all metabolites had the highest content at the mature stage. The Changes in volatile compounds were significantly dependent on the growth stage and increased with the growth stage. It was worth noting that the shell breaking of the fruiting body was the critical turning point for the synthesis and accumulation of volatile compounds. In addition, volatile compounds, mainly containing 6-undecyl alcohol, α-terpine-7-al, 2, 4-decenol, and 2-cyano-2-ethyl-butanamide, might co-regulate flavor formation of *Phallus impudicus* during growth stage through the synergistic action of other chemical components.

CRediT authorship contribution statement

Huijuan Liu, literature collection, manuscript written-review, editing and supervision; Zhifei Cheng, sample collection, language check and manuscript supervision; Jiao Xie, sample collection and carried out the experiment, had fund acquisition and manuscript revise and supervision.

Declaration of competing interest

The authors declare that they have no known competing financial interests or personal relationships that could have appeared to influence the work reported in this paper.

Data availability

Data will be made available on request.

Acknowledgements

This research was supported by Guizhou Provincial Science and Technology Projects (ZK [2022] 365 and ZK [2022] 391); High-level talents start-up fund project of Guizhou Medical University ([2021] 007).

Appendix A. Supplementary data

Supplementary data to this article can be found online at https://doi.org/10.1016/j.fochx.2024.101288.

References

Aisala, H., Sola, J., Hopia, A., Linderborg, K. M., & Sandell, M. (2019). Odor-contributing volatile compounds of wild edible nordic mushrooms analyzed with HS-SPME-GC-MS and HS-SPME-GC-O/FID. *Food Chemistry, 283*, 566–578.

Bao, G. F., Mu, L. Q., & Wang, Y. (2023). Effect of different accumulative temperate zones in Heilongjiang on glycine soja metabolites as analyzed by non-target metabolomics. *Molecules, 28*(8), 3296.

Cao, L. P., Zhang, Q., Miao, R. Y., Lin, J. B., Feng, R. C., Ni, Y. Q., & Zhao, X. (2023). Application of omics technology in the research on edible fungi. *Current Research in Food Science, 6*, Article 100430.

Cho, D. B., Seo, H. Y., & Kim, K. S. (2003). Analysis of the volatile flavor compounds produced during the growth stages of the shiitake mushrooms (lentinus edodes). *Journal of Food Science & Nutrition, 8*(4), 306–314.

Dickschat, J. S., Celik, E., & Brock, N. (2018). Volatiles from three genome sequenced fungi from the genus *Aspergillus*. *Beilstein Journal of Organic Chemistry, 14*, 900–910.

Dombrowski, J. E., Kronmiller, B. A., Hollenbeck, V. G., Rhodes, A. C., Henning, J. A., & Martin, R. C. (2019). Transcriptome analysis of the model grass *Lolium temulentum* exposed to green leaf volatiles. *BMC Plant Biology, 19*, 222.

Dunkel, A., Steinhaus, M., Kotthoff, M., Nowak, B., Krautwurst, D., Schieberle, P., & Schieberle, T. (2014). Nature' s chemical signatures in human olfaction: A foodborne perspective for future biotechnology. *An gewandte Chemie International Edition, 53*(28), 7124–7143.

Feng, T., Yang, M. Y., Ma, B., Zhao, Y., Zhuang, H. N., Zhang, J. S., & Chen, D. (2021). Volatile profiles of two genotype *Agaricus bisporus* species at different growth stages. *Food Research International, 140*, Article 109761.

Gómez, I., Laveg González, R., Tejedor-Calvo, E., Pérez Clavijo, M., & Carrasco, J. (2022). Odor profile of four cultivated and freeze-dried edible mushrooms by using sensory panel, electronic nose and GC-MS. *Journal of Fungi, 8*(9), 953.

Granato, D., Santos, J. S., Escher, G. B., Ferreira, B. L., & Maggio, R. M. (2018). Use of principal component analysis (PCA) and hierarchical cluster analysis (HCA) for multivariate association between bioactive compounds and functional properties in foods: A critical perspective. *Trends in Food Science & Technology, 72*, 83–90.

Grosshauser, S., & Schieberle, P. (2013). Characterization of the key odorants in panfried white mushrooms (Agaricus bisporus L.) by means of molecular sensory science: Comparison with the raw mushroom tissue. *Journal of Agricultural and Food Chemistry, 61*(16), 3804–3813.

Gupta, A., Jayaprakash, & Shinde, B. (2016). Immunopharmacological activity of medicinal plants against *Aristolochia* bracteolate and *Phallus impudicus*. *Journal of Biomedical and Pharmaceutical Research, 5*(5), 9–15.

Hosaka, K., Bates, S. T., Beever, R. E., Castellano, M. A., Colgan-III, W., Domínguez, L. S., & Trappe, J. M. (2006). Molecular phylogenetics of the gomphoid-phalloid fungi with an establishment of the new subclass phallomycetidae and two new orders. *Mycologia, 98*(6), 949–959.

Hou, J. X., Liang, L., & Wang, Y. X. (2020). Volatile composition changes in navel orange at different growth stages by HS-SPM-GC-MS. *Food Research International, 136*, Article 109333.

Huang, W. J., Fang, S. M., Wang, J., Zhou, C., Luo, Y. H., Yu, Y. L., & Ning, J. M. (2022). Sensomics analysis of the effect of the withering method on the aroma components of Keemun black tea. *Food Chemisty, 395*, Article 133549.

Khan, A. R., Fiaz, M., Khan, R. A., Wahab, Z., Khan, J. B., Khan, I., & Jan-Khan, M. W. (2020). Anti-oxidant and hypoglyceamic potential of phallus impudicus (l. ex pers) (stink horn) mushroom in alloxan induced diabetic rats. *Journal of Critical Reviews, 7*(18), 4180–4185.

Kuznecova, G., Jegina, K., Kuznecovs, S., & Kuznecovs, I. (2007). P151 *Phallus impudicus* in thromboprophlyaxis in breast cancer patients undergoing chemotherapy and hormonal treatment. *The Breast, 16*, S56.

Li, W., Li, R., Chen, W. C., Feng, J., Wu, D., Zhang, Z., & Yang, Y. (2022). The anabolism of sulphur aroma volatiles responds to enzymatic and non-enzymatic reactions during the drying process of shiitake mushrooms. *Food Chemistry, 371*, Article 131123.

Li, L., Zuo, Z. T., & Wang, Y. Z. (2022). Practical qualitative evaluation and screening of potential biomarkers for different parts of *Wolfiporia cocos* using machine learning and network pharmacology. *Frontiers in Microbiology, 13*, Article 931967.

Mostafa, S., Wang, Y., Zeng, W., & Jin, B. (2022). Floral scents and fruit aromas: Functions, compositions, Biosynthesis, and regulation. *Frontiers in Plant Science, 13*, Article 860157.

Pudil, F., Uvira, R., & Janda, V. (2014). Volatile compounds in stinkhorn (phallus impudicus l. Ex pers.) at different stages of growth. *European Scientific Journal, 10*(9), 163–171.

Shen, S. S., Wu, H. T., Li, T. H., Sun, H. R., Wang, Y. J., & Niang, J. M. (2023). Formation of aroma characteristics driven by volatile components during long-term storage of an tea. *Food Chemistry, 411*, Article 135487.

Shou, K.X. (2020). Constituents analysis, activity evaluation of *Phallus Impudicus* L. and purification, structural properties of its polysaccharides. Master Thesis, *Guizhou Medical University*, the China. 4-5pp, pp. 12.

Sun, L. B., Zhang, Z. Y., Xin, G., Sun, B. X., & Xu, H. R. (2020). Advances in umami taste and aroma of edible mushrooms. *Trends in Food Science & Technology, 96*, 176–187.

Sun, T., Jiang, H., Yang, K., Li, X. K., Wang, S. Y., Yao, H. Y., & Sun, D. F. (2022). Nutritional function and flavor evaluation of a new soybean beverage based on *Naematelia aurantialba* fermentation. *Foods, 11*(3), 272.

Tagkouli, D., Bekiaris, G., Pantazi, S., Anastasopoulou, M. E., Koutrotsios, G., Mallouchos, A., & Kalogeropoulos, N. (2021). Volatile profiling of *Pleurotus eryngii* and *Pleurotus ostreatus* mushrooms cultivated on agricultural and agro-industrial by-products. *Foods, 10*(6), 1287.

Thévenot, E. A., Roux, A., Xu, Y., Ezan, E., & Christophe, J. (2015). Analysis of the human adult urinary metabolome variations with age, body mass index, and gender by implementing a comprehensive workflow for univariate and OPLS statistical analyses. *Journal of Proteome Research, 14*(8), 3322–3335.

Tietel, Z., & Masaphy, S. (2018). True morels (morchella)-nutritional and phytochemical composition, health benefits and flavor: A review. *Critical Reviews in Food Science and Nutrition, 58*(11), 1888–1901.

Vyacheslav, B., Alexey, B., Aliaksandr, A., Valentina, M., Tatyana, P., Aliaksandar, K., & Mikolaj, T. (2019). Polysaccharides of mushroom *Phallus impudicus* mycelium: Immunomodulating and wound healing properties. *Modern Food Science and Technology, 35*(9), 30–37.

Xie, J., Cao, Q., Wang, W. J., Zhang, H. Y., & Deng, B. (2023). Understanding changes in volatile compounds and fatty acids of Jincheng orange peel oil at different growth stages using GC-MS. *Journal of Integrative Agriculture, 22*(7), 2282–2294.

Yao, F., Gao, H., Yin, C. M., Shi, D. F., & Fan, X. Z. (2023). Effect of different cooking methods on the bioactive components, color, texture, microstructure, and volatiles of Shiitake Mushrooms. *Foods, 12*(13), 2573.

Yuan, H., Cao, G., Hou, X., Huang, M., Du, P., Tan, T., & Luo, J. (2022). Development of a widely targeted volatilomics method for profiling volatilomes in plants. *Molecular Plant, 15*(1), 189–202.

Zhang, S. (2015). Study on the antimicrobial preservative effect of *Dictyophora echinovlvata* and *Phallus impudicus*. *Master Thesis, Zhejiang Agriculture & Forestry University, the China., 3*, pp.